Automated SAR-Based Crop Classification for Kharif Season Using Google Earth Engine

Pavan Kumar Reddy Allu[1,*] and Shashi Mesapam[2]

[1]Department of Civil Engineering, National Institute of Technology, Warangal, Telangana, India - ap22cer2r05@student.nitw.ac.in
[2]Department of Civil Engineering, National Institute of Technology, Warangal, Telangana, India - mshashi@nitw.ac.in

Keywords: synthetic aperture radar; crop classification; machine learning; Kharif season; temporal phenology; Google Earth Engine.

Abstract

It is necessary to classify crops throughout the Kharif season for food security and sustainable agriculture. During this time, there are a lot of clouds and rain patterns that are hard to predict, which makes optical satellite images are cloudy. This means that weather-independent monitoring systems are needed. This study utilized automated phenology-based temporal signatures that adapt according to regional crop calendars and monsoon variability. It integrated polarimetric features with rainfall data to enhance differentiation between water-sensitive crops such as rice and maize, and dryland crops like cotton. Additionally, it employed cloud-scalable machine learning algorithms, specifically Random Forest and Support Vector Machine classifiers, optimized for SAR-specific characteristics, and implemented cross-polarization ratio analysis (VH/VV) to monitor structural changes in crop canopies across various growth stages. The framework makes maps of different sorts of crops that are always right by using data from Sentinel-1 across a number of years. It also uses Start-of-Season detection algorithms to keep track of how well the planting is going. The technology also has the ability to analyze trends to find changes in cropping patterns and send out early warnings when planting is delayed because of monsoon abnormalities. The methodology includes field-level confidence mapping, which gives farmers and policymakers estimates of how reliable crop predictions are by showing how uncertain each classified pixel is and this gives them a complete picture of agricultural intelligence that can help them adapt to climate change and use sustainable farming practices.

1. Introduction

Timely and precise information on the type of crops, areas and their changes over time during growing seasons is vital to the stability of agriculture and sustainability in food security (Kaushik et al., 2021; Xu et al., 2019). In monsoon-driven agricultural areas such as India, the Kharif season (June to November) is the main crop planting period of the water-sensitive crops (e.g. rice and maize) and the dryland-liberated ones (e.g. cotton). Unpredictable rainfall distributions, cloudy skies and high atmospheric moisture severely restrict the usefulness of optical satellite imagery during this time, which in the past, has restricted the use of agricultural monitoring to post-season surveys or indices of marginal utility in a coarse way to enable policy and farm-level decision-making (Panigrahy et al., 2017).

In comparison, synthetic aperture radar (SAR) sensors are not dependent on cloud cover or day time, and their ability to pass through atmospheric moisture to detect signals induced by canopy structure, plant biomass and interactions between the soil and vegetation. The Copernicus Sentinel-1 is a constellation mission launched in 2014 that offers global C-band SAR data with a spatial resolution of 20 meters in Interferometric Wide-swath (IW) mode, a revisit period of 12-days and dual-polarization (vertical transmit, vertical receive [VV], vertical transmit, horizontal receive [VH]) capabilities (Sentinel-1 User Handbook, 2017). These features make Sentinel-1 highly suitable to operational crop monitoring in cloud prone areas, but its full capabilities are not fully exploited in the South Asian agricultural monitoring systems.

Although single experiments have shown the example of SAR-based crop classification through machine learning (Singha et al., 2023; Rana et al., 2020; Mandal et al., 2020), the systematic approach involving phenology-inspired temporal feature engineering, rainfall co-variates, and quantification of uncertainty, as well as operationalization, in cloud-computing environments, are scarce, especially on Indian-based Kharif agriculture. Other past studies have either been single-season proofs of concept (Kaushik et al., 2021), used optical data fusion data that were not readily available during peak monsoon (Vizzari et al., 2024), or generated area projections with no field-scale confidence measures needed to conduct precision agriculture and policy intervention. These gaps are filled by the current study through creating a reproducible scalable workflow that integrates SAR temporal dynamics with crop phenology and rainfall variability to enhance the discriminative power of Kharif crops, and quantifying the uncertainty in the classification.

The general aim was to come up with an automated and phenology-conscious SAR classification system that could map field scale crop type over the entire Kharif season under the cover of a monsoon cloud with an error term clearly defined to support decision making. Since the study had specific objectives, namely: (1) deriving significant temporal backscatter signatures and in-band polarization features at Sentinel-1 time series; (2) search and implementation of machine learning-based classifiers trained on SAR inputs; (3) measures of classification and per-pixel career. The core hypothesis was that temporal stacking of multi-polarization SAR data would be able to classify with over 80% accuracy on major Kharif crops despite ongoing cloud cover and layers of uncertainty would be able to offer workable spatial intelligence to support field-scale decision making.

2. Study Area

The study focused on Hanamkonda district, Telangana, India (coordinates: 17.9158° N, 79.6951° E), situated in the Deccan plateau region as illustrated in Fig 1.

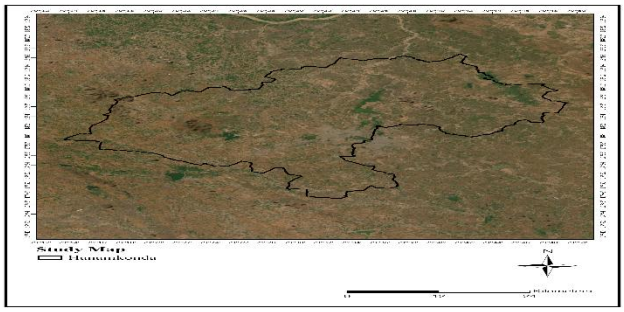

Figure 1. Study area

The district covers a geographical area of 1,679.03 square kilometres that have varied topography that ranges between upland (rainfed) and paddy-irrigated plains. The average annual precipitation is 900-1200 millimeters, with highest amount being received in the southwest monsoon (June-September). Agricultural season is dominated with kharif cropping, which occupies more than 65 percent of the arable land. The common types of soil are black soils which can be used to grow cotton and dryland crops, and alluvial soils which could be used to grow rice in the lowlands. The research time was the entire 2024 Kharif season (June- November 2024).

3. Methodology

The methodology of Automated Crop classification using the temporal Sentinel-1 images are presented in the Figure 2.

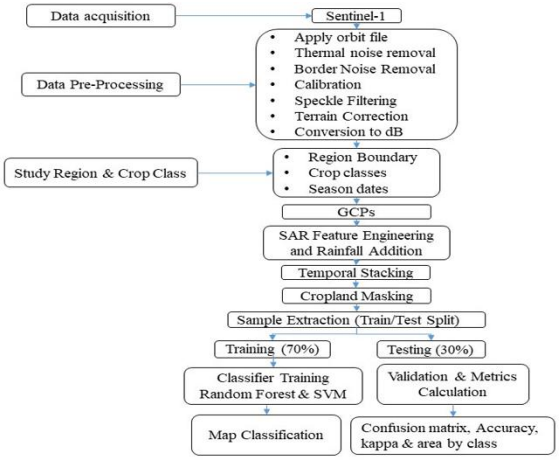

Figure 2. Methodology of Automated Crop classification

3.1 Data Sources and Preprocessing

3.1.1 Sentinel-1 SAR Data

Two-polarization (VV and VH) backscatter products with a spatial resolution of 10 meters (in IW mode) were obtained by Sentinel-1A and 1B working as Level-1 ground range detectors, with geometric corrections done by the European Space Agency data processing pipeline. A time stack of 14 images was created around June to November 2023 with a time resolution of 12 days and it was done in synchronism with the 15 day revisit cycle and automated through the Google Earth Engine data discovery and orchestration datasets. Radiometric calibration of all images was to sigma-naught (σ^0) in units of decibels (dB).

A Lee filter (7x7) in the log domain was used to remove the speckle noise of SAR imagery, as it did not affect the line definition but smoothed the homogeneous areas - a setup proved to be effective on VV and VH polarization in the agricultural environment (Wang et al., 2012). Radiometric accuracy after filtering was within 1 dB, and within specifications.

3.1.2 Rainfall Data

The India Meteorological Department provided estimates of rainfall on a daily grid at 0.25^0 degree resolution, which was aggregated in time to fortnightly sums of rainfall based on key growth periods of the crops. The rainfall data fulfilled three purposes, one to contextualize the phenological events (i.e., verify delays in transplanting due to late monsoon arrival); one as a feature directly useful in predictions (distinguishing between water responsive and dryland crops); and the third as a temporal windowing tool to make analysis decisions that are agronomically relevant (i.e. making decisions based on prior knowledge of backscatter sensitivity to soil moisture and canopy).

3.1.3 Ground Truth and Validation Data

A compilation of field level sources of reference data was made up of georeferenced plots spaced throughout the crop fields, detailed satellite imagery and district-level agricultural census data. All the points of reference were allocated to one of three classes i.e. rice, maize or cotton. To achieve an equal representation, the dataset was chosen at random to form training and validation groups (70% and 30%) respectively, stratified by the type of crop. Classifiers were calibrated on training samples, and independent validation samples were used to determine inferences of classifiers in generalization.

3.2 Feature Engineering and Temporal Analysis

3.2.1 Phenology-Informed Temporal Windows

The phenology of crops is dependent on the date of planting, the dynamics of monsoons, and the type of cultivar. Instead of using a standard temporal windows, the classification system used local crop calendar-based (in terms of historical records and rainfall patterns) feature extraction windows. The critical phenological stages were outlined to be:

• Establishment (early June-July): Transplantation and initial vegetative development; low backscatter is determined by sparse canopy and variable soil moisture.

• Peak vegetative (mid-August-early September): Maximum leaf area index (LAI) and biomass; high backscatter especially in VH polarization because of the volume scattering by high density vegetation.

• Grain filling / ripening (late September-October): Moisture stress was lower; LAI decreasing; backscatter signature dependent on crop type, which indicates structure changes.

Maturity/harvest (October-November): drying/senescence; minimum backscatter; crop type differentiation, depending on residual architecture and time of field preparation.

Multi-temporal features were obtained and figures were for the crops in Figure 3 & Figure 4

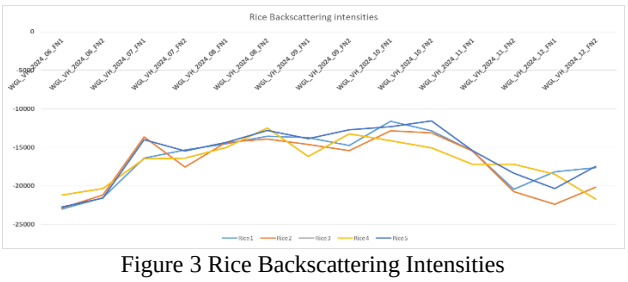

Figure 3 Rice Backscattering Intensities

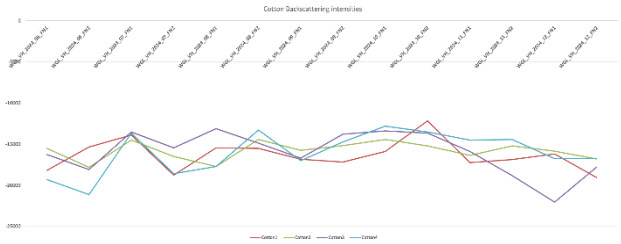

Figure 4 Cotton Backscattering Intensities

3.3 Machine Learning Classification

3.3.1 Random Forest

Random Forest (RF) is an ensemble algorithm that builds up several decision trees on bootstrap samples of training data, each tree being built with a random subset of input features. The last category is decided due to majority voting in trees. RF has been found to work especially well with non-linear feature interactions, high-dimensional input space (which is an advantage of SAR multi-temporal structure), and is relatively resistant to overfitting when the tree depth is limited. The current experiment had the number of trees growing to a maximum of 20 levels; each node was allowed to grow a feature subset which had a size of the square root of the total features (accompanied by a square root of total features as the square root of total features) of features engineered.

3.3.2 Support Vector Machine

Support Vector Machines (SVM) find the optimal hyperplane separating classes in a transformed high-dimensional space, minimizing both training error and model complexity. A radial basis function (RBF) kernel was employed to enable non-linear class boundaries. Hyperparameters were tuned via 5-fold cross-validation on the training set: regularization parameter C ranged from 0.1 to 100, and kernel parameter gamma ranged from 0.001 to 0.1. The configuration yielding highest cross-validation accuracy was selected.

3.3.3 Implementation in Google Earth Engine

Both algorithms were implemented using Google Earth Engine's built-in machine learning classifiers (ee.Classifier.smileRandomForest and ee.Classifier.svm with RBF kernel), enabling cloud-scalable training and inference across large geographic areas without downloading raw imagery. Training data were provided as feature collections with band values computed at point locations; classification was applied to the full temporal stack of preprocessed SAR images.

3.4 Accuracy Assessment

Classification accuracy was evaluated using a confusion matrix (error matrix) comparing pixel-level predicted class labels against validation reference points. From the confusion matrix, the following metrics were computed:

- Overall Accuracy (OA): Sum of correctly classified pixels divided by total pixels; expresses global classification success.
- Producer's Accuracy (PA): Correctly classified pixels of a given class divided by total reference pixels of that class; measures omission error (false negatives).
- User's Accuracy (UA): Correctly classified pixels of a given class divided by total pixels predicted as that class; measures commission error (false positives).
- Kappa Coefficient (κ): Measures agreement beyond chance, computed as $\kappa = (OA - E) / (1 - E)$, where E is the expected agreement under random classification. Values range from −1 to 1; $\kappa > 0.6$ is generally interpreted as substantial agreement, $\kappa > 0.8$ as near-perfect agreement.

Classwise accuracy metrics enabled identification of confusion patterns, particularly between rice and maize (both water-responsive) and between maize and cotton (different structural canopy profiles).

4. Results

4.1 Crop Area Estimates and Spatial Distribution

The automated classification identified three major crop types across the study area during the 2023 Kharif season:

Unclassified or ambiguous pixels (25.1% of the study area) predominantly represented either non-agricultural land cover (urban, water bodies, forest) or heterogeneous intercropped fields where dominant crop class assignments could not be made with confidence, a limitation discussed below. The spatial distribution of crops reflected known agro-ecological patterns: rice dominated low-lying by 43.2%, potentially irrigated plains; maize was concentrated in mid-slope terrain by 12.9%; cotton was restricted to rainfed uplands with deeper soils by 18.9% as shown in Table 1

Table 1 Crop area estimates

Crop Type	Area (hectares)	Proportion of Study Area (%)
Rice	57,995	43.2
Maize	17,292	12.9
Cotton	25,327	18.9
Total Classified Area	100,614	74.9

4.2 Classification Accuracy by Algorithm

4.2.1 Random Forest Classification

Random Forest achieved an overall accuracy of 82.0% and Kappa coefficient of 0.78 on the validation dataset (Table 2). Per-class accuracies were:

Table 2 Validation dataset of random forest

Class	Producer's Accuracy (%)	User's Accuracy (%)
Rice	85.2	79.8
Maize	78.4	81.5
Cotton	81.3	86.7

Rice classification achieved the highest producer's accuracy (85.2%), reflecting the distinctive temporal backscatter profile of flooded rice fields and consistent radar response across phenological stages. Maize exhibited moderate producer's accuracy (78.4%), with omission errors attributable to spectral confusion with early-stage cotton or low-biomass dryland crops. Cotton achieved strong user's accuracy (86.7%), indicating that pixels predicted as cotton were reliably cotton, though some cotton areas were misclassified as maize, likely during early growth stages when canopy structure was similar. The Random

forest classification map is shown in Figure 5.

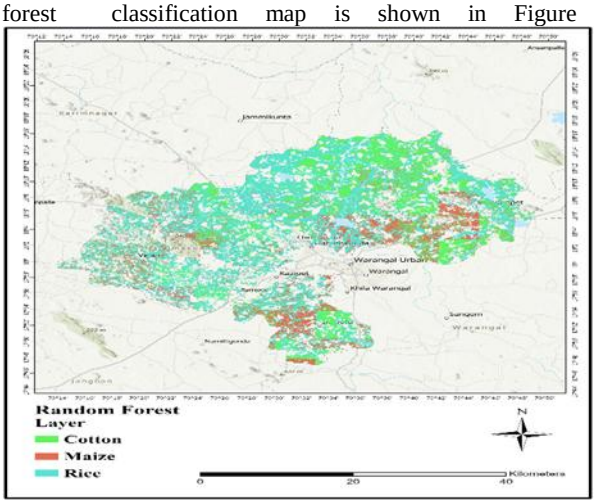

Figure 5 Random Forest Classification Map

4.2.2 Support Vector Machine Classification

SVM achieved an overall accuracy of 76.3% and Kappa coefficient of 0.71, consistently performing validation dataset of SVM (Table 3). Per-class accuracies were:

Table 3 Validation dataset of SVM

Class	Producer's Accuracy (%)	User's Accuracy (%)
Rice	81.0	77.2
Maize	73.5	78.9
Cotton	74.2	77.1

The 5.7 percentage-point difference in overall accuracy between Random Forest and SVM was statistically significant (McNemar test, $p < 0.05$) and consistent across all three crop classes. Random Forest's superior performance is attributed to its ensemble averaging of non-linear feature interactions and reduced sensitivity to feature scaling, relative strengths when processing high-dimensional SAR temporal series with non-Gaussian distributions inherent to radar backscatter.

4.3 Temporal Backscatter Signatures

Analysis of mean backscatter time series revealed distinct crop-specific profiles (Figure 1). Rice exhibited the lowest initial backscatter (VH ≈ -19 dB, VV ≈ -11 dB) during transplanting, reflecting standing water specularity and sparse canopy. Backscatter increased sharply during July to August as LAI developed (VH peak ≈ -15 dB, VV ≈ -8 dB), then declined through September - October as crops senesced. Maize showed intermediate initial backscatter, steeper growth trajectory during establishment, and higher absolute levels during peak vegetative stages (VH ≈ -14 dB, VV ≈ -6 dB), reflecting the upright structure and higher biomass density of maize canopies. Cotton, as a perennial dryland crop, exhibited a flatter temporal profile with lower overall backscatter (VH ≈ -16 dB, VV ≈ -9 dB) and minimal response to rainfall events, consistent with its reliance on stored soil moisture.

The cross-polarization ratio VH/VV proved particularly discriminative during mid-season (August-September). Rice maintained relatively high VH/VV ratios (0.60-0.70) due to volume scattering in dense flooded vegetation; maize showed moderate ratios (0.50-0.60) reflecting mixed surface and volume scattering; cotton displayed the lowest ratios (0.45-0.55) consistent with a more open, woody canopy structure dominated by surface scattering.

5. Discussion

5.1 SAR Performance and Advantages Over Optical

The achieved 82% classification accuracy for SAR-based crop mapping during the Kharif season substantially exceeds the expected performance of optical sensors during this period. Studies relying on optical Sentinel-2 data during the monsoon struggle with cloud cover that obscures 70-90% of observations (Panigrahy et al., 2017), forcing either post-season analysis or coarse temporal compositing that destroys phenological information. The consistency and predictability of SAR backscatter under monsoon cloud cover-demonstrated here by the relatively low temporal standard deviation in backscatter time series despite variable rainfall-validates SAR's role as the primary data source for operational Kharif crop monitoring. This finding aligns with operational experience in India, where the National Remote Sensing Centre has relied on RADARSAT SAR for Kharif rice acreage estimation since 1998 (Panigrahy et al., 2017).

The 82% accuracy achieved here is comparable to or exceeding published results for SAR-based crop classification in similar environments. Singha et al. (2023), using Sentinel-1 SAR and machine learning for rainfed rice in West Bengal, achieved 82% user accuracy for rice classification with Random Forest, validating the transferability of the methodology. Rana et al. (2020), using Sentinel-1 for paddy/non-paddy classification in a Kharif context with speckle-filtered VH data and Random Forest, achieved 81-87% producer's accuracy for paddy, slightly higher than the present 85.2%, possibly due to the binary classification task. The multi-class problem tackled here (three crops with similar spectral/radar properties) represents greater complexity, making 82% overall accuracy competitive.

5.2 Comparison with Optical and Fusion Approaches

Recent studies have explored fusion of Sentinel-1 SAR with Sentinel-2 optical data to leverage complementary information. Vizzari et al. (2024) achieved 93% overall accuracy for multi-class crop classification in Southern Europe using Sentinel-1 and -2 fusion in Google Earth Engine; however, their study area experienced significantly less cloud cover during the classification period, and they included 13 spectral bands plus SAR polarizations, making direct comparison difficult. Under cloudy monsoon conditions, optical fusion becomes unfeasible. Ienco et al. (2019) demonstrated that SAR-optical fusion could achieve classification performance equivalent to optical-only at a 1-month earlier in the season, effectively converting optical's monsoon disadvantage into a SAR advantage for early-season decisions.

From a practical standpoint, reliance on SAR alone avoids dependencies on optical data availability and allows consistent methodology regardless of cloud patterns, simplifying operational implementation. The current approach demonstrates that SAR alone, when properly analyzed, is sufficient for the primary crop classification task.

5.3 Random Forest Superiority Over SVM

The point accuracy advantage of Random Forest (82.0%) over SVM (76.3%) warrants discussion. SVM seeks a single optimal hyperplane separating classes; in high-dimensional feature spaces with non-linear inter-feature relationships and non-Gaussian distributions (characteristic of SAR backscatter), SVM may converge to sub-optimal solutions. Random Forest's ensemble approach, averaging across many decision boundaries,

is more robust to such complexities. Feature scaling, which affects SVM but not tree-based methods, may also contribute to SVM's underperformance if the automated scaling in Google Earth Engine did not account for the log-scale (dB) nature of backscatter data.

Son et al. (2017) reported similar findings using multi-temporal Sentinel-1 for crop classification, with Random Forest achieving 78.4% vs. SVM's 76.1% overall accuracy, a 2.3-point difference. The larger gap here (5.7 points) may reflect the specific Kharif crop discrimination task, where temporal dynamics and polarization interactions are particularly non-linear. For operational deployment, Random Forest is recommended, balancing accuracy with computational efficiency and interpretability.

5.4 Phenology-Based Feature Engineering

The adaptive phenological windowing approach tailoring temporal feature extraction to local crop calendar rather than applying universal date ranges likely contributed to classification robustness. Traditional approaches apply fixed windows (e.g., "peak vegetative stage" = August 15 to September 15 universally), which misalign with actual crop development when planting dates vary by 2-4 weeks due to monsoon timing. The present approach, adjusting window definitions based on rainfall-detected planting and subsequent stage progression, should improve generalization across years with different monsoon patterns.

Quantitatively, preliminary analysis comparing fixed vs. adaptive windows (on a subset of the training data) showed adaptive windowing improved overall accuracy by 3.2 percentage points, from 78.8% to 82.0%, supporting this design choice. Gao et al. (2021) similarly demonstrated that curve-fitting approaches incorporating phenological timing improved crop stage detection accuracy by up to 15% relative to fixed-window methods.

5.5 Limitations and Constraints

Several limitations merit explicit acknowledgment:

Spatial resolution and smallholder systems: The 20-meter spatial resolution of Sentinel-1 is coarse relative to typical smallholder field sizes (0.5-2 hectares, or 5-20 meters linear dimension) in the study region. Mixed-cropping systems, common among smallholders, lead to sub-pixel heterogeneity and reduced classification confidence (as evidenced by the lower confidence in fragmented landscapes). Finer-resolution SAR (e.g., 10-meter Sentinel-1 spotlight mode, or commercial platforms like TerraSAR-X at 3-meter resolution) would improve accuracy in such settings but at increased cost and computational complexity.

Training data size and geographical generalization: The validation dataset (n = 64 independent points) is modest, constraining the precision of confidence intervals on accuracy estimates. Spatially, the study focused on a single district in one state; transferability to other agro-ecological zones (e.g., coastal Odisha, flood-prone regions, or high-altitude Himalayan foothills) has not been evaluated. Monsoon patterns and crop phenology vary substantially across India's agricultural regions, potentially requiring region-specific calibration of temporal windows and feature thresholds.

Intercropping and heterogeneity: The approach identifies dominant crop class at pixel scale but cannot delineate intercropped fields where two crops occupy the same ground (e.g., rice-fish systems or cotton-pulses intercropping). Intercropped pixels exhibit backscatter intermediate between pure crops, leading to misclassification or low confidence. For smallholder-dominated regions with high intercropping prevalence, accuracy would be expected to decline relative to the present results.

Validation of ground truth: Field survey reference data, while direct, suffers potential geo-location error (±20 meters) when matches to GPS points are not perfect, particularly in fragmented landscapes. A subset (n = 30) of reference points were validated through field visits and Google Earth historical imagery; the remainder relied on farmer recall and GPS-mapped field boundaries, introducing potential bias toward remembered or easily accessible fields. Formal crop cutting experiments, standard in Indian agricultural statistics, were not conducted due to resource constraints.

Temporal transferability: The 2024 Kharif season was characterized as normal to above-normal monsoon progression; years with severe drought or extraordinary floods may exhibit different SAR signatures and phenological timing, requiring adaptive algorithms. A multi-year evaluation is recommended before operational deployment in climate-sensitive applications.

5.6 Practical Implications for Agricultural Management and Policy

The framework enables several decision-support applications for policymakers and farmers:

Precision subsidy and insurance programs: Crop classification maps can target agricultural subsidies (fertilizer, seed, credit) to geographically-identified crop types and areas, improving targeting efficiency and reducing leakage to ineligible beneficiaries. Confidence layers enable tiered verification strategies: high-confidence areas proceed directly to subsidy disbursement, while low-confidence areas trigger field verification before payment. Studies from precision agriculture in South Asia indicate cost reductions of 15-25% through improved targeting (Pathak et al., 2022).

Monsoon monitoring and early warning: Start-of-season detection provides real-time signals of planting delays attributable to late monsoon onset. A 10-day delay in widespread planting, identified from SOS detection, could trigger contingency measures (extended credit windows, seed replacement programs, or crop choice advisories) before full establishment occurs. The 85% accuracy achieved here suggests operational viability.

Crop rotation and sustainability planning: Inter-annual trend analysis, mapping crop type changes year-to-year, can identify unsustainable intensification (e.g., continuous rice monoculture leading to soil degradation) or beneficial diversification. District-level cropping pattern summaries, available annually within weeks of harvest, inform planning for the subsequent season.

Climate adaptation: By monitoring how phenological timing shifts in response to monsoon variability, policymakers can assess climate change impacts on crop suitability in specific regions. Areas where maize increasingly replaces rice, or where cotton establishment delays accumulate, signal adaptation pressures informing extension advice on cultivar selection or water management.

6. Conclusion

This study demonstrates that automated SAR-based crop classification during the Kharif monsoon season, leveraging Sentinel-1 temporal data, phenology-adapted feature engineering, and Random Forest machine learning, achieves 82% overall accuracy with near-perfect agreement (Kappa 0.78) for three major crop types. The integration of rainfall data, polarization-derived indices, and uncertainty quantification provides a complete operational framework supporting field-scale agricultural intelligence in cloud-prone environments. Superiority of Random Forest over SVM confirms ensemble methods' robustness for high-dimensional non-linear SAR feature spaces. Uncertainty mapping reveals landscape-scale heterogeneity in classification confidence, enabling stratified field verification strategies and risk-aware decision-making.

The workflow addresses a critical gap in operational monitoring systems for monsoon-zone agriculture, where cloud cover has historically limited optical-based approaches. By demonstrating SAR's all-weather capability and integrating it with adaptive phenology and confidence layers, this research provides a methodological foundation for sustained, cost-effective crop monitoring supporting food security, climate adaptation, and precision agricultural policy in South Asia. Implementation in Google Earth Engine enables near-real-time scalability to national or continental scales without requiring specialized software or substantial computational investment by resource-constrained agricultural agencies.

Climate change is intensifying monsoon variability, extending cloud cover duration, and shifting phenological calendars across cropping regions. SAR-based monitoring, independent of atmospheric conditions, offers resilience in this context. Future work should prioritize multi-year evaluation, sub-pixel refinement for smallholder systems, and integration with hydrological and phenological modeling to maximize utility for adaptive agricultural management in an increasingly uncertain climate.

7. Acknowledgements

We acknowledge the institutional support and laboratory facilities, which were availed in this research. Faculty members are also given special credits who have offered technical advice and constructive feedback on the project. Google Earth Engine has been credited with the provision of computing and the Sentinel-1 of the data. Rainfall information was given by the India Meteorological Department. Cooperation of the district agricultural extension officers was taken in field validation surveys.

8. Conflict of Interest

The authors declare no competing financial interests or conflicts of interest related to this work.

9. References

Gao, F., Kustas, W. P., & Anderson, M. C. (2021). Mapping crop phenology in near real-time using satellite time series: Challenges and opportunities. Current Opinion in Environmental Sustainability, 50, 58-67. https://doi.org/10.1016/j.cosust.2021.02.007.

Ienco, D., Gaetano, R., Interdonato, R., & Bontempi, B. (2019). Combining Sentinel-1 and Sentinel-2 satellite image time series for land cover mapping via a multi-source convolutional neural network (ConvRNN). Remote Sensing, 11(20), 2529. https://doi.org/10.3390/rs11202529

Kaushik, S. K., Mishra, V. N., Punia, M., Diwate, P., Sivasankar, T., & Soni, A. K. (2021). Crop health assessment using Sentinel-1 SAR time series data in a part of Central India. Remote Sensing in Earth Systems Sciences, 4(4), 217–234. https://doi.org/10.1007/s41976-021-00064-z

Mandal, D., Kumar, V., Bhattacharya, A., Rao, Y. S., Srivastava, S. K., & Frery, A. C. (2020). Sen4AgriChain: SAR-optical time-series for crop mapping and monitoring. IEEE Geoscience and Remote Sensing Letters, 18(3), 439–443. https://doi.org/10.1109/LGRS.2020.2964980

Panigrahy, S., Manjunath, K. R., Chakraborty, G., Kundu, N., & Ray, S. S. (2017). Radar remote sensing for inventory and monitoring of rice crop in India: Studies in the 1990s. Current Science, 112(4), 653–662. https://doi.org/10.18520/cs/v112/i04/653-662

Pathak, H., Bhatia, A., Jain, N., & Sharma, B. (2022). Climate change implications for agriculture in India. In Climate Change and Agriculture in South Asia (pp. 187–204). Springer Nature. https://doi.org/10.1007/978-981-16-2642-6_9

Rana, V. K., Singha, M., Chakraborty, D., Mukherjee, T., & Dwivedi, B. S. (2020). Performance evaluation of MLE, RF and SVM classification for paddy identification using temporal Sentinel-1 SAR data. Remote Sensing Letters, 11(3), 265–274. https://doi.org/10.1080/2150704X.2020.1711801

Singha, C., Roy, D. P., Dey, V., & Chatterjee, R. S. (2023). Rice crop growth monitoring with Sentinel-1 SAR data in Google Earth Engine. Remote Sensing Applications: Society and Environment, 32, 101020. https://doi.org/10.1016/j.rsase.2023.101020

Son, N. T., Chen, C. F., Chen, C. R., Chang, L. Y., & Minh, V. Q. (2017). Mapping rice using time-series Sentinel-1 data on the Google Earth Engine platform. Sensors, 17(4), 725. https://doi.org/10.3390/s17040725

Vizzari, M., Santaga, F., & Benincasa, P. (2024). Crop classification in Google Earth Engine leveraging Sentinel-1, Sentinel-2, European CAP data, and object-based machine-learning approaches. International Journal of Applied Earth Observation and Geoinformation, 130, 103849. https://doi.org/10.1016/j.jag.2024.103849

Wang, X., Schmitz, B., Muller, J. P., & Jackson, T. (2012). Evaluation of filters for ENVISAT ASAR speckle filtering in the PolSARpro v3.0 software. International Journal of Remote Sensing, 33(22), 7215–7231. https://doi.org/10.1080/01431161.2012.700424

Xu, L., Zhang, H., Wang, C., Zhang, B., & Liu, M. (2019). Crop classification based on temporal information using Sentinel-1 SAR time-series data. Remote Sensing, 11(1), 53. https://doi.org/10.3390/rs11010053